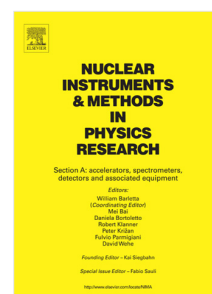


Journal Pre-proof

Cherenkov diffraction radiation emissions from single electrons and positrons on a fused silica radiator

Silas Ruhrberg Estevez, Tobias Baumgartner, Johann Bahl,
Thomas Lehrach, Tobias Thole, Benildur Nickel, Philipp Loewe,
Lukas Hildebrandt, Cristóvão Beirão da Cruz E Silva, Paul Schütze,
Markus Joos



PII: S0168-9002(23)00277-2
DOI: <https://doi.org/10.1016/j.nima.2023.168287>
Reference: NIMA 168287

To appear in: *Nuclear Inst. and Methods in Physics Research, A*

Received date: 2 October 2022
Revised date: 28 February 2023
Accepted date: 6 April 2023

Please cite this article as: S.R. Estevez, T. Baumgartner, J. Bahl et al., Cherenkov diffraction radiation emissions from single electrons and positrons on a fused silica radiator, *Nuclear Inst. and Methods in Physics Research, A* (2023), doi: <https://doi.org/10.1016/j.nima.2023.168287>.

This is a PDF file of an article that has undergone enhancements after acceptance, such as the addition of a cover page and metadata, and formatting for readability, but it is not yet the definitive version of record. This version will undergo additional copyediting, typesetting and review before it is published in its final form, but we are providing this version to give early visibility of the article. Please note that, during the production process, errors may be discovered which could affect the content, and all legal disclaimers that apply to the journal pertain.

© 2023 The Author(s). Published by Elsevier B.V. This is an open access article under the CC BY license (<http://creativecommons.org/licenses/by/4.0/>).

Cherenkov Diffraction Radiation Emissions from Single Electrons and Positrons on a Fused Silica Radiator

Silas Ruhrberg Estevez^a, Tobias Baumgartner^a, Johann Bahl^a, Thomas Lehrach^a, Tobias Thole^a, Benildur Nickel^a, Philipp Loewe^a, Lukas Hildebrandt^a, Cristóvão Beirão da Cruz E Silva^c, Paul Schütze^b, Markus Joos^{c,*}

^a*Werner-von-Siemens-Gymnasium, Beskidenstr. 1, 14129 Berlin, Germany*

^b*Deutsches Elektronen-Synchrotron DESY, Notkestr. 85, 22607 Hamburg, Germany*

^c*CERN, Esplanade des Particules 1, Meyrin, 1217 Geneva, Switzerland*

Abstract

Beam diagnostics are crucial for smooth accelerator operations. Many techniques rely on instrumentation in which the beam properties are significantly affected by the measurement. Novel approaches aim to use Cherenkov Diffraction Radiation (ChDR) for non-invasive diagnostics. Unlike regular Cherenkov Radiation, the charged particles do not have to move inside of the medium, but it is sufficient for them to move in its vicinity as long as they are faster than the speed of light in the medium. Changes to the beam properties due to ChDR measurements are consequently negligible. To examine ChDR emission under different conditions, we placed a fused silica radiator in the DESY II Test Beam. We observed increases in ChDR intensity for electron and positron momenta between 1 GeV c^{-1} and 5 GeV c^{-1} . Additionally, we found a larger photon yield for electrons than positrons for increasing particle momenta. However, the significance of these measurements is strongly

*Corresponding author: markus.joos@cern.ch (Markus Joos)

limited by the accuracy of the conversion from the measured signal to absolute photon numbers. The results suggest a need for further research into the ChDR generation by electrons and positrons and may find application in the design of future beam diagnostic devices.

Keywords: CERN, DESY, Test beam, Beamline for Schools, Cherenkov Radiation, ChDR

1. Introduction

Cherenkov radiation is light produced by charged particles when they pass through an optically transparent medium at speeds exceeding the speed of light in that medium [1]. It was first observed experimentally in 1937 by P. A. Cherenkov [2]. He shared the Nobel Prize in Physics 1958 with I. M. Frank and I. Y. Tamm who developed a theoretical model of the phenomenon [3]. The model was improved by Ginzburg and Frank to show the emission originated from dielectric material regions parallel to the particle motion [4]. The radiation emission has since been calculated using electromagnetic field eigenvalues [5] and Di Francia expansions [6]. More recent work has described ChDR generation in different scenarios [7] [8].

In the last few years, the existence of ChDR has been proven experimentally [9]. ChDR can be emitted if an ultrarelativistic charged particle moves in the vicinity of a dielectric medium [10]. The atoms of the medium get polarized by the electric field of the ultrarelativistic charged particle, oscillate, and thereby emit light [11] at a characteristic Cherenkov angle $\cos(\theta) = \frac{1}{\beta n}$, where β is the relativistic factor and n is the refractive index of the material.

19 For fused silica ($n = 1.46$) and ultrarelativistic particles ($\beta \approx 1$) the angle is
 20 approximately 46.8° [12].

21

22 ChDR is polarized as it arises from fields of charged particles inducing dy-
 23 namic polarization currents at the air-radiator interface [13]. The angular
 24 distribution is determined by the spatial arrangement of the particle and ra-
 25 diator [13]. However, ChDR differs from regular Cherenkov Radiation in that
 26 both horizontal and vertical components are measurable as only a fraction
 27 of the radiation cone is measured [14]. Differences in radiation between the
 28 horizontal and vertical direction, depending on the arrangement of beam and
 29 radiator, have been observed [9]. Previous experiments have shown an expo-
 30 nential decay of ChDR intensity for increasing distances from the dielectric
 31 radiator which they determined to be in good agreement with predictions
 32 from polarization radiation theory [9]. Increased ChDR emission rates for
 33 electrons at 5.3 GeV compared to 2.1 GeV have also been observed [14] but
 34 to our knowledge no detailed analysis of the effect of particle momentum or
 35 energy on ChDR generation has been performed.

36

37 ChDR has been proposed to be a method for non-invasive beam diagnos-
 38 tics as the particles do not physically interact with the radiator [14]. Beam
 39 position and bunch length monitors exploiting ChDR emission have been
 40 trialled successfully [10] [15]. In this article we present the results of placing
 41 a dielectric radiator in the vicinity of a particle beam at the DESY II Test
 42 Beam Facility and measuring the emission rates of photons under different

conditions¹. The Test Beam facility allows measurement of ChDR generated by single particles while previous work has focused on particle bunches [9][14]. We focus on a comparison of the emissions from electrons and positrons in the same setup. To our knowledge this has not been done before as previous experiments were conducted on circular colliders where electrons and positrons travel in opposite directions [14].

2. Methods

2.1. Experimental setup

The DESY II Test Beam Facility offers positron and electron beams with selectable momenta from 1 GeV c^{-1} to 6 GeV c^{-1} [18]. A maximum particle rate of $10 \times 10^3 \text{ Hz}$ is reached at around 2 GeV c^{-1} [17]. The Test Beam is generated by double conversion of the DESY II synchrotron beam [18]. Bremsstrahlung is produced from $7 \mu\text{m}$ carbon primary targets held inside the synchrotron beam. The Bremsstrahlung then creates electron-positron-pairs on a secondary metal target with dimension $45 \text{ mm} \times 60 \text{ mm}$ [18]. The particles subsequently pass through a dipole magnet, which allows selection of particle type and momentum. A $10 \text{ mm} \times 20 \text{ mm}$ collimator constrains the beam before it traverses the experimental setup.

¹All experiments were conducted by high school students under expert guidance as part of the Beamline for Schools (BL4S) competition 2020. BL4S is a worldwide competition offered by CERN since 2014 that provides high school students with the opportunity to conduct their own experiments at a state-of-the-art particle accelerator [16]. In the years 2019 - 2021, BL4S was co-organized by DESY and held mostly at their facilities in Hamburg due to the Long Shutdown 2 at CERN [17].

61

62 The experimental setup comprises trigger scintillators, a beam telescope
 63 consisting of six silicon pixel detectors [19] that are permanently installed at
 64 DESY, a photomultiplier tube (PMT) and a fused silica radiator. A sketch
 65 of the arrangement of the components of the experimental setup can be seen
 66 in Figure 1. The beam telescope features a high position resolution, in the
 67 order of a few micrometers, and low material budget, which enables the re-
 68 construction of particle tracks at the given momentum range and thus an
 69 estimation on the relative particle distance to the radiator. It is used in a
 70 configuration with three detector planes each before and behind the radi-
 71 ator. In addition, a pair of scintillators is utilised as input to the trigger
 72 system. The PMT (ET enterprises 9813QKB) was operated at 1650 V for all
 73 experiments and has a spectral response from 165 nm to 630 nm [20]. This is
 74 similar to camera systems with a wavelength of 300 nm – 700 nm that have
 75 been used previously to detect ChDR [9].

76

77 The radiator is positioned partially inside the beam, such that the center
 78 of the beam spot is located at the edge of the radiator. Thus, a large portion
 79 of particles passes in close proximity of the radiator. Inevitably, a signifi-
 80 cant fraction of particles also traverses the radiator, leading to emission of
 81 non-diffraction Cherenkov radiation. To reduce contamination from ambient
 82 light, the PMT and radiator were placed in an aluminum box, painted black
 83 on the inside. The box was placed on linear motion stages for an alignment
 84 transverse to the beam, while the radiator itself was mounted on a rota-
 85 tion stage for an angular alignment parallel to the beam. Figure 2 shows

the setup inside the box including the radiator with alignment stage and the PMT. Beam windows covered with black tape were added to reduce the material budget while maintaining the blocking of ambient light. The PMT was, optionally, equipped with polarization filters in order to study radiation polarization.

2.2. Radiator

Right-angled trapezoid prism radiators made of high purity fused silica (SiO_2) were obtained from Heraeus [21] and CERN. The unique prism geometry of the radiators allows for ChDR generated over the entire length of the radiator to reach the PMT. Figure 3 shows how light generated along the entire length of the radiator can undergo internal reflections to reach the wedge shaped end of the radiator. A reflective coating at the 21.8° angled surface was applied to enforce the radiation exiting the radiator perpendicularly to the opposite surface. To determine the QDC signal baseline, a small piece of aluminum foil, blocking the light exiting the radiator and entering the PMT, was temporarily applied over this area of the radiator.

2.3. Triggering & Data Acquisition

Two assemblies of scintillators, light guide and PMT, were used for triggering purposes. These scintillators were powered and their signals interpreted by the Trigger Logic Unit (TLU) [22], which is used for coincidence detection on discriminated input signals with a programmable threshold. The TLU in turn formed a particle trigger signal and performs a trigger-busy-handshake with all detectors, inhibiting any further trigger signals from being distributed while any detector is indicating a busy signal. In consequence of

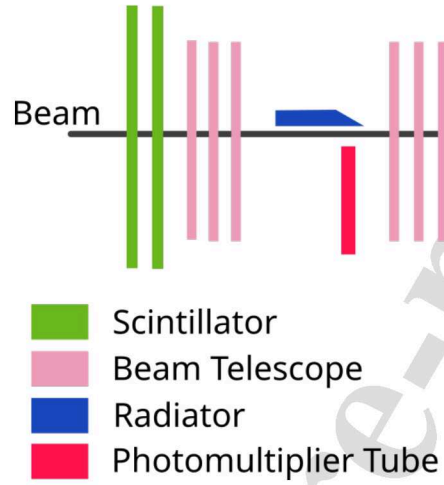


Figure 1: Sketch of the experimental setup at the DESY II Test beam facility showing the relative positions of the detectors used and the radiator.

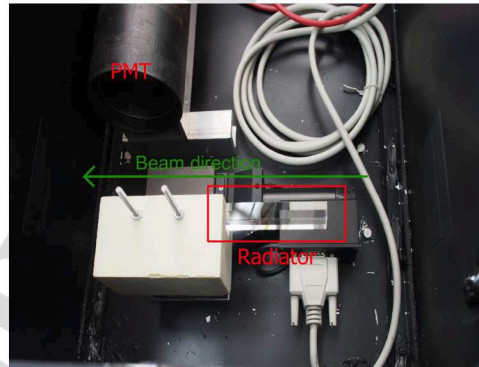


Figure 2: Picture of the radiator mounted on a rotation stage next to the PMT inside a black painted aluminum box.

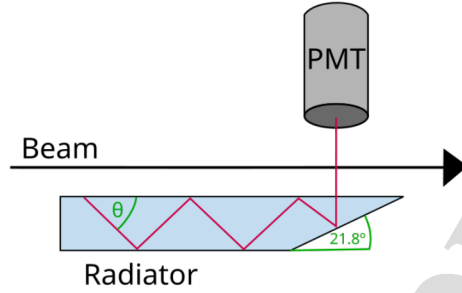


Figure 3: Sketch of ChDR emission in a long dielectric radiator based on a design previously described for non-invasive beam diagnostics [10].

110 a trigger, the telescope data was recorded, storing the data as well as the trig-
 111 ger numbers to the disk. The PMT signal was digitized via a 12 bit charge to
 112 digital converter (QDC) of the type CAEN V965 [23]. For this, an integration
 113 window was created through a pulse generator, initiated by the trigger signal
 114 and with a width that was empirically determined to cover the full duration
 115 of all PMT pulses. The QDC raised a busy signal while the integration is in
 116 process. The data acquisition was controlled via the EUDAQ2 data acquisi-
 117 tion framework [24]. This software enabled the initialization, configuration
 118 and control of the telescope, the QDC, the scintillators, the TLU, and the
 119 motion and rotation stages via dedicated configuration files. It furthermore
 120 featured so-called data collectors, which have the task of writing the data to
 121 disk.

122 2.4. Data Analysis

123 2.4.1. Determination of radiator boundary

124 The data was analysed using ROOT [25] and PyRoot in Jupyter Note-
 125 book [26]. The radiator boundary was determined using a Material Budget

126 Image (MBI). The MBI used is a two-dimensional mapping representing the
 127 amount of material traversed by relativistic charged particles [27]. The kink
 128 angle, the angle between the tracking lines obtained before and after pass-
 129 ing through the setup, is used as an estimate of the amount of material the
 130 particle traversed [28]. The MBI used is the projection of the kink angle for
 131 each particle to a plane within the radiator length approximately halfway
 132 between the first and sixth pixel detector of the beam telescope. A difference
 133 in the average kink angle between the radiator and the surrounding air can
 134 be seen in the MBI in Figure 4. The boundary of the radiator is defined by
 135 the points, in (x, y) coordinates, where the average kink angle is half way
 136 between that of air and that of the radiator. The radiator boundary was
 137 then estimated by fitting of a straight line through these points, resulting in
 138 a close to vertical line. During analysis, the track position at the MBI plane
 139 is calculated and the impact parameter is the distance of the track position
 140 to the fitted line.

141 The boundary measurement was performed for each group of runs where
 142 the exact position of the radiator could have changed from a previous group
 143 of runs, which could happen due to manual interventions on the setup. The
 144 standard error of the radiator boundary position was determined from the
 145 variance of the (x, y) values compared to the fitted line. On average, the
 146 standard error was about 0.02mm. We decided to use 0.035mm for the
 147 uncertainty of the radiator boundary position from the line fitting as the
 148 bin size used in the fit was 0.035 mm. The radiator boundary position was
 149 defined for each run as the straight line position subtracted by the value of
 150 the standard error.

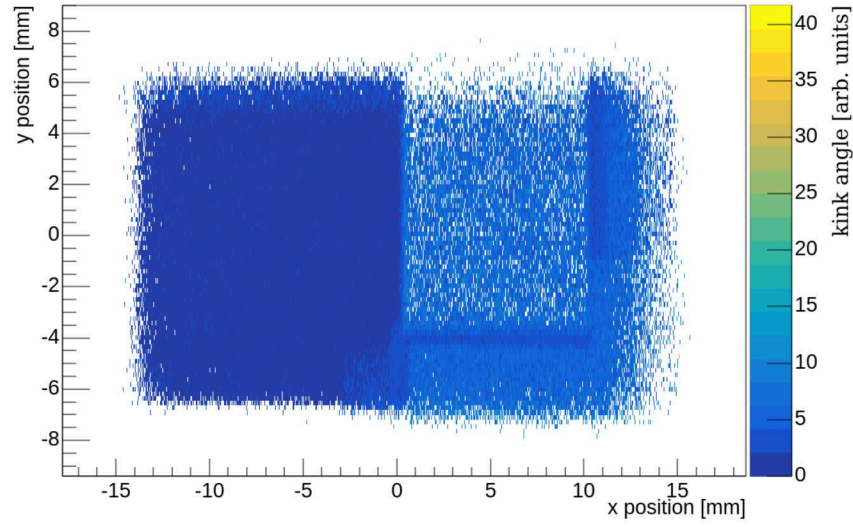


Figure 4: X-Y projection material budget image of the beam profile kink angle. The left section, in dark blue corresponds to air; the low statistics region with large kink angles, in the top right area, corresponds to the radiator; the region below and to the right of the radiator with slightly increased kink angles compared to the air region, corresponds to the support structure of the radiator; a small gap of air, between the radiator and support structure can also be observed in the darker colors, reflecting a lower kink angle, as expected from the geometric design of the mechanical support; a faint silhouette of a plastic screw and washer from the support structure can also be observed on the bottom, with kink angles between those of air and the support structure itself.

151 2.4.2. Analysis of particle tracks

152 The particle hits were clustered and tracked using the corrvreckan li-
 153 brary [29]. The track of the particles in the region of the radiator was calcu-
 154 lated by reconstructing the pathway of the particle with straight lines fitted
 155 through the clusters before and after the radiator. The particle tracks were
 156 used to calculate which particles passed inside the radiator, thus producing
 157 non-diffraction Cherenkov radiation, and which particles passed outside the
 158 radiator, thus being candidates for producing diffraction Cherenkov radia-
 159 tion. This information is summarised, for each particle, in the impact pa-
 160 rameter which is defined as the distance of the track to the radiator surface
 161 (as defined in Section 2.4.1), with positive values indicating a position inside
 162 the radiator and negative values a position outside the radiator. Events with
 163 multiple tracks are removed from analysis. To reduce contamination in the
 164 ChDR output from particles that underwent scattering, we have excluded
 165 all particles where there is a distance between the predicted values from the
 166 upstream and downstream line fitting greater than 0.15 mm, with a distance
 167 between a cluster on a single detector and the predicted linear fit greater
 168 than 0.2 mm or with an upstream angle greater than 0.005 rad from further
 169 analysis.

170 2.4.3. Comparison of positron and electron beam angular spread

171 Since the impact parameter is determined at the MBI plane, particles
 172 with large impact angles may traverse the radiator at the edges and produce
 173 non-diffraction Cherenkov radiation. Analysis of the angular spread in x -
 174 direction of the fitted particle tracks for 2 GeV c^{-1} and 5 GeV c^{-1} suggests
 175 that there are no significant differences between positrons and electrons (see

176 Fig. 5).

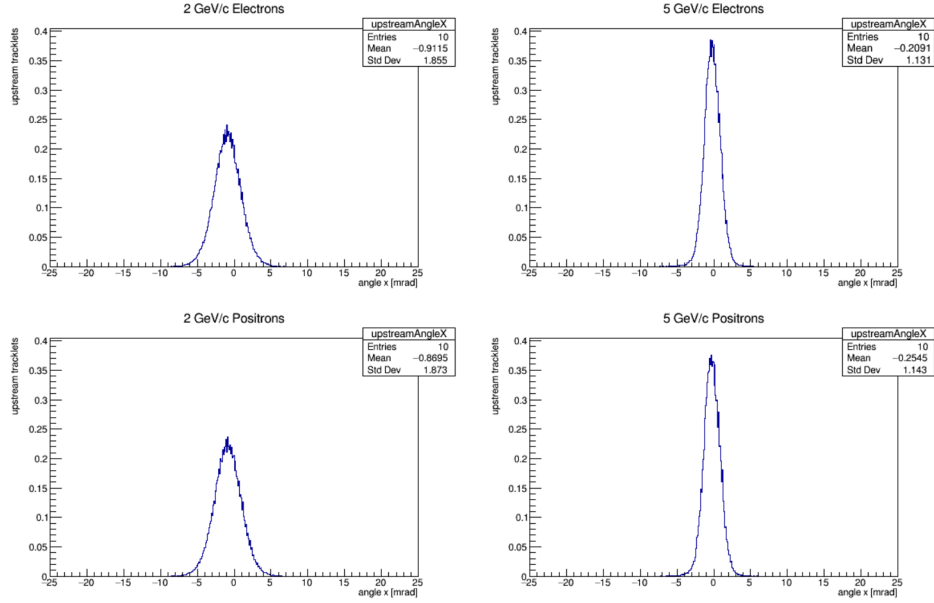


Figure 5: The distribution of angles of the particle tracks before the radiator for electrons (top) and positrons (bottom) at 2 GeV c^{-1} (left) and 5 GeV c^{-1} (right). No significant differences of the angular spread between electron and positron beams were observed.

177 The angular spread of the particle tracks decreases as the momentum
 178 increases, as expected since the effect of multiple scattering should also de-
 179 crease.

180 2.4.4. Analysis of ChDR emission

181 The average pulse amplitude measured from the PMT was plotted against
 182 impact parameter for electrons and positrons respectively (see Fig. 6 and 7).
 183 For the initial analysis, the arbitrary QDC output unit values were used
 184 as a measure of light intensity. The dotted line in the plot denotes the

185 bias current pedestal, an offset value arising from the QDC measurement
 186 process. Events with distances from the radiator boundary greater than
 187 1.2 mm were excluded from the analysis as they were considered to be too far
 188 away. The graph obtained was then modelled by an exponential function [9]
 189 of type $a + b \cdot e^{cx}$ fitted over 1 mm, ending at a value that corresponds to the
 190 uncertainty of the radiator edge (see Fig. 6 and 7). The parameters and χ^2 of
 191 the functions for different particle types and momenta are given in Table 1.
 192 To obtain a number representative of the total photon production for specific
 193 conditions, the fitted function was integrated in the interval. To account for
 194 the pedestal, the integral of the pedestal in the same interval was subtracted
 195 from this number. Errors of the exponential fit of the data and the subsequent
 196 integration were calculated using the ErrorIntegral macro from ROOT [30].
 197 To analyse the contamination from light other than Cherenkov radiation,
 198 a run with aluminum foil blocking light generated inside the radiator from
 199 entering the PMT was performed and analysed in the same way (see Fig. 8),
 200 no significant contamination was observed and the baseline value ($69.52 \pm$
 201 0.38) is compatible with a pure pedestal background (69.23 ± 0.52). The
 202 6 GeV c^{-1} electron measurement was excluded from the analysis because after
 203 tracking there was an insufficient number of data points with accurate tracks
 204 (see Fig. 6). However, the experiment with 6 GeV c^{-1} positrons had enough
 205 data.

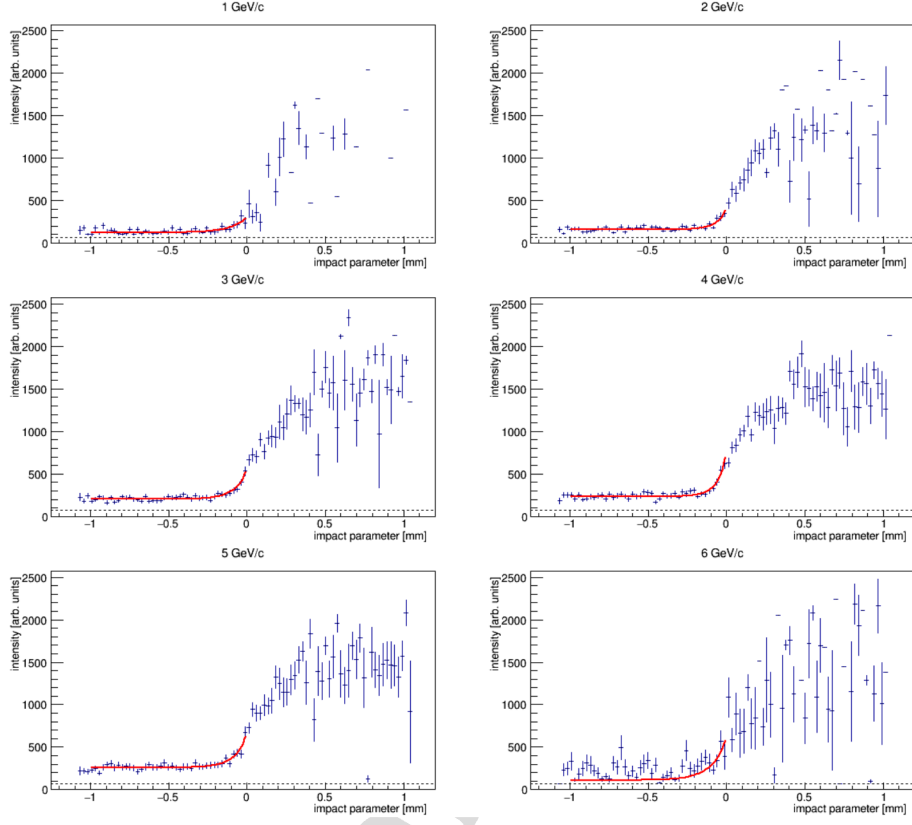


Figure 6: Histograms of the average light intensity for electrons in arbitrary QDC units as a function of the track impact parameter for beam momenta between 1 GeV c^{-1} and 6 GeV c^{-1} . The region immediately outside the radiator is fitted with an exponential.

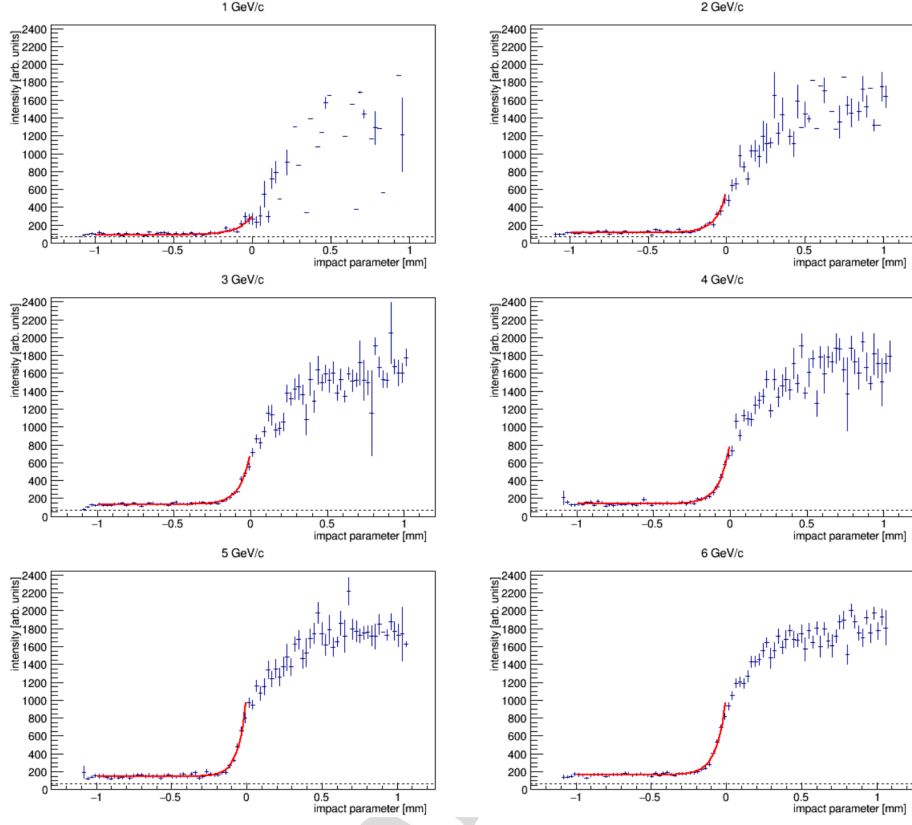


Figure 7: Histograms of the average light intensity for positrons in arbitrary QDC units as a function of the track impact parameter for beam momenta between 1 GeV c^{-1} and 6 GeV c^{-1} . The region immediately outside the radiator is fitted with an exponential.

Beam	a	b	c	χ^2/ndf
1 GeV/c e^-	1.23×10^2	1.69×10^2	0.97×10^1	1.00
1 GeV/c e^+	0.92×10^2	2.04×10^2	1.10×10^1	1.83
2 GeV/c e^-	1.59×10^2	2.39×10^2	1.64×10^1	1.54
2 GeV/c e^+	1.15×10^2	4.51×10^2	1.46×10^1	1.78
3 GeV/c e^-	2.02×10^2	3.33×10^2	1.30×10^1	1.04
3 GeV/c e^+	1.34×10^2	5.66×10^2	1.45×10^1	1.14
4 GeV/c e^-	2.34×10^2	4.95×10^2	1.72×10^1	1.53
4 GeV/c e^+	1.37×10^2	6.76×10^2	1.43×10^1	0.91
5 GeV/c e^-	2.59×10^2	3.86×10^2	1.32×10^1	0.91
5 GeV/c e^+	1.47×10^2	8.95×10^2	1.80×10^1	0.95
6 GeV/c e^+	1.64×10^2	8.62×10^2	1.56×10^1	1.21

Table 1: Parameters of the exponential fit of photon emission as a function of impact parameter for different particle types and momenta. The exponential function used was of type $a + b \cdot e^{cx}$.

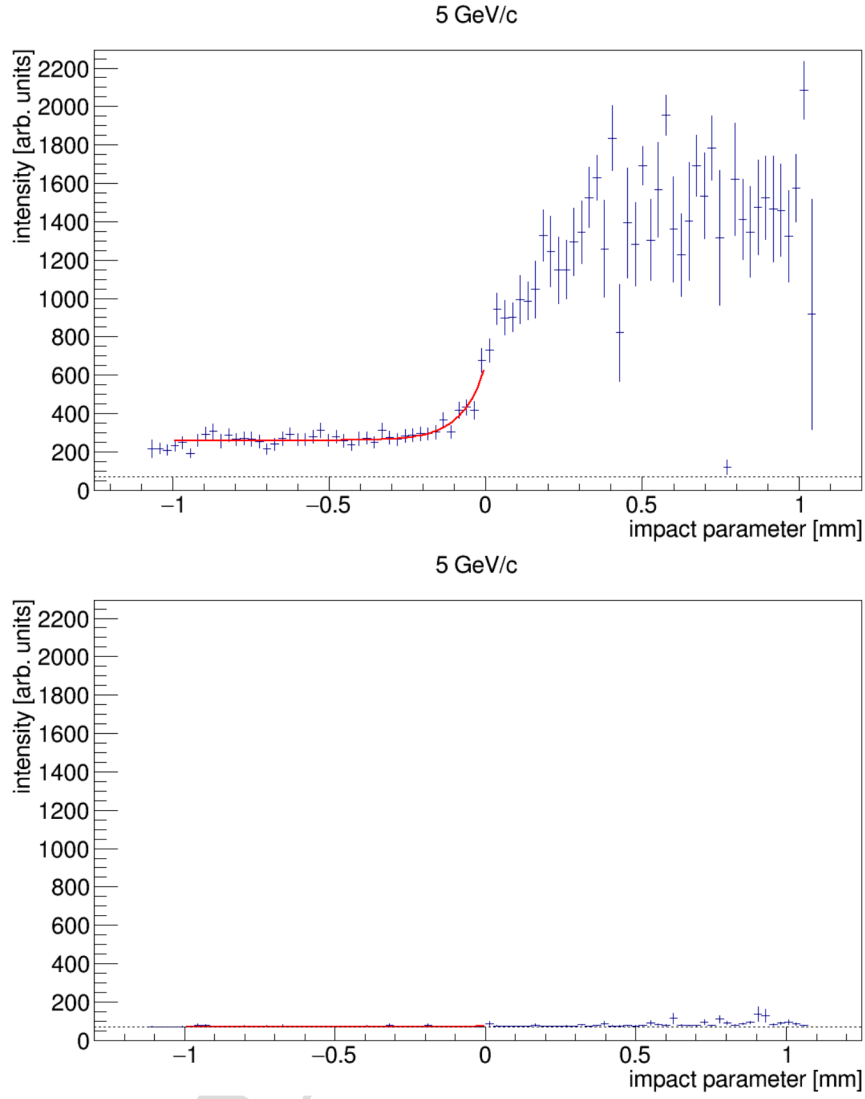


Figure 8: Histograms of the light intensity in arbitrary QDC units as a function of the track impact parameter for 5 GeV c^{-1} electrons without (top) and with (bottom) an aluminum foil blocking light emission from the radiator. The region immediately outside the radiator is fitted with an exponential. Blocking the photon exit point on the radiator reduces both non-diffraction Cherenkov Radiation and ChDR detection to negligible levels.

206 2.4.5. QDC signal calibration

207 A pulsed green LED in front of the PMT was used to calibrate the QDC
 208 output. The distance of the LED as well as current, voltage and duration of
 209 the electrical pulses applied to the LED were controlled such that less than 1
 210 in 10 pulses resulted in a signal being produced by the PMT. The number of
 211 photons reaching the PMT can be assumed to be a Poisson distribution and
 212 in these conditions a Poisson with a mean less than 0.1. Under these circum-
 213 stances, the probability of having more than one photon is vanishingly small,
 214 therefore, the few pulses from the PMT must be from single photon events.
 215 By fitting a superposition of two Gaussian functions to the peak in the signal
 216 that corresponds to single photons and the bias current pedestal an estimate
 217 of the conversion factor from arbitrary QDC units to number of photons can
 218 be obtained. Figure 9 shows the intensity distribution of the QDC output in
 219 response to a flashing LED and the Gaussian fits of the data. The measured
 220 conversion factor was found to be $(7.48 \pm 3.63) \text{ QDCunits photon}^{-1}$. The un-
 221 certainty of the conversion factor was calculated using Gauss' law of error
 222 propagation and the standard deviations of the individual Gauss functions
 223 used in the fitting.

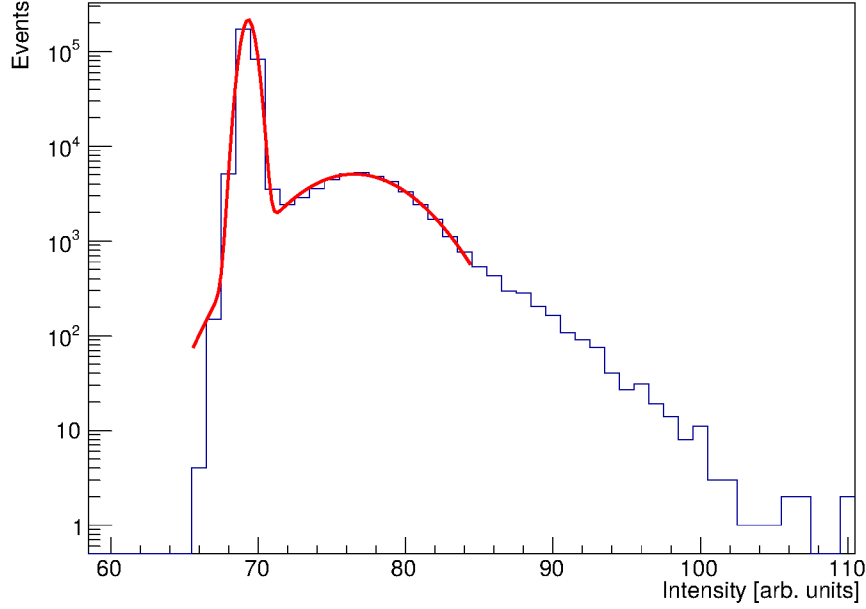


Figure 9: Measured intensity distribution from a flashing single photon LED (blue line) fitted with a superposition of two Gaussian functions (red line).

2.4.6. Analysis of total photon emission

Finally, the converted values of the respective integrals were plotted as a function of particle momentum for both electrons and positrons (see Fig. ??). We report the emission of ChDR using the integral of the average amount of photons emitted per particle in the 1 mm interval of interest with the unit [photon mm]. The uncertainty of the photon count was calculated with Gauss' law of error propagation using the uncertainties of the photon conversion and the previously determined error of the integral.

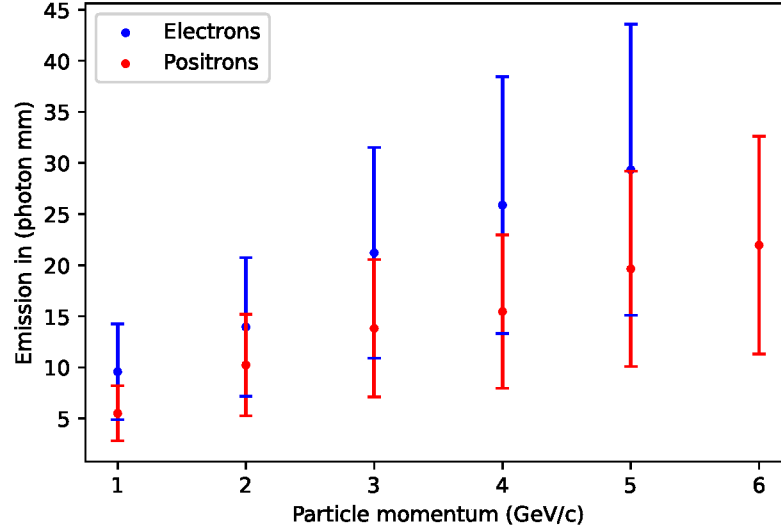


Figure 10: Values of the converted integral of the exponential fits as a function of beam momentum.

3. Results and Discussion

Comparing the experiments with and without aluminum foil suggests a significant increase in photon emission due to Cherenkov Radiation from an interaction between the charged particles and the radiator (see Fig. 8). Application of the foil over the radiator reduced the measured light intensities at all impact parameters to negligible levels. Tracking the particles then allows accurate discrimination between photons generated from non-diffraction Cherenkov Radiation and Cherenkov Diffraction Radiation. We are therefore confident to have detected ChDR. This is supported by our observation of a increase in light emission between 1 GeV c^{-1} and 6 GeV c^{-1} for positrons

242 and 1 GeV c^{-1} and 5 GeV c^{-1} for electrons when comparing the values of the
 243 integral of the exponential fit (see Fig. 10). We also observed significantly
 244 higher QDC outputs for electrons compared to positrons. However, there is
 245 no significant difference in the generation of photons as the QDC units to
 246 photon conversion is not very accurate (see Fig. 10). Inside the radiator
 247 we observe much higher emissions of light from non-diffraction Cherenkov
 248 radiation, although these events are affected by the particle tracking cuts,
 249 being removed by the tracking exclusion criteria.

250 To further characterise the radiation, we measured the photon generation
 251 for various orientations of a polarization filter placed over the PMT. The
 252 results from this data indicate that ChDR generated in our setup has a
 253 higher horizontal than vertical polarization component both at 3 GeV c^{-1} and
 254 5 GeV c^{-1} (see Table 2). Higher emissions of vertically polarized photons for
 255 a radiator placed above the beam have been reported in the literature [14].
 256 As the radiator in our experiment was placed on the side of the beam, our
 257 results agree with this observation. The observed light intensity also did not
 258 drop to negligible levels when the polarization filter was oriented at 90° to
 259 the main polarization direction suggesting both polarization components are
 260 present. This seems in agreement with theoretical predictions [14].

261 We also evaluated a short radiator from CERN on top of the Heraeus ra-
 262 diator we used for the main experiments. The dimensions were $5 \text{ cm} \times 1 \text{ cm} \times$
 263 0.5 cm and $15 \text{ cm} \times 1.5 \text{ cm} \times 1 \text{ cm}$, respectively. The CERN radiator was pre-
 264 viously used in other experiments and exhibited some degree of yellowing of
 265 the medium, visible by eye, which may affect the light yield of this radiator.
 266 Previous experiments suggested a linear increase in light emission for longer

267 radiators [10]. We found an increase in light emission (see Table 3) for the
 268 larger radiator, but this was higher than the tripling the theory predicts for
 269 a radiator with trice the length [10]. The results of the short radiator also
 270 do not support the hypothesis that electrons emit significantly more photons
 271 than positrons as there was no significant difference in light emission. The
 272 results in the longer radiator may be misleading as the longer radiator could
 273 make the setup more sensitive to background Cherenkov radiation produced
 274 in air or the black tape input windows. There is also a possibility of pho-
 275 ton emission due to ultrarelativistic particles that is not ChDR. This could
 276 also explain why we see much higher photon emission in the longer radia-
 277 tor compared to the theoretical prediction. It is however not clear why this
 278 would lead to an increase in photon production for electrons compared to
 279 positrons. We also show that there are no significant differences between the
 280 angular spreads of the respective particle beams, which could have caused
 281 increases in light yield, especially for the longer radiator. We also could not
 282 verify if there are differences in beam momentum and momentum spread of
 283 the DESY Test Beam with the setup used. The deviation from the linear
 284 increase in light emission as a function of radiator length is likely due to the
 285 yellowing presented by the CERN radiator. Differences in thickness, width or
 286 manufacturing of the radiators may also have influenced the measurements.

287 4. Conclusion

288 We show that ChDR emission increases with particle momentum between
 289 1 GeV c^{-1} and 5 GeV c^{-1} for both positrons and electrons. Unlike previous
 290 experiments on circular colliders, we measured emission by both particle

Polarisation	3 GeV c ⁻¹ (photon mm)	5 GeV c ⁻¹ (photon mm)
Vertical	0.36 ± 0.17	0.36 ± 0.17
Vertical +45° ccw	0.56 ± 0.27	0.73 ± 0.36
Horizontal	2.10 ± 1.02	2.64 ± 1.28
Horizontal +45° ccw	1.00 ± 0.49	1.28 ± 0.62

Table 2: Integrated ChDR emissions for 3 GeV c⁻¹ and 5 GeV c⁻¹ electrons in the 1 mm interval using different orientations of the polarisation filters.

Beam	Small radiator (photon mm)	Large radiator (photon mm)
2 GeV e ⁻	1.02 ± 0.49	13.96 ± 6.78
3 GeV e ⁻	1.13 ± 0.46	21.21 ± 10.30
2 GeV e ⁺	0.95 ± 0.54	10.22 ± 4.97
3 GeV e ⁺	1.19 ± 0.58	13.83 ± 6.71

Table 3: Integrated ChDR emissions for 2 GeV c⁻¹ and 3 GeV c⁻¹ electrons and positrons in the 1 mm interval using two different radiators.

types in the same setup. We report significantly higher QDC measurements for electrons compared to positrons between 1 GeV c^{-1} and 5 GeV c^{-1} but this difference is not significant after converting the measurements to photon counts. To our knowledge, differences in emission rates of electrons and positrons have not been reported for ChDR or non-diffraction Cherenkov Radiation. Further experiments to investigate this possible difference are needed because there is uncertainty if the photon conversion in our setup is not accurate enough or there is actually no significant difference. Our results also indicate that ChDR may be useful for monitoring the momenta of particle beams, as the light emissions are a function of the particle momentum for both positrons and electrons.

5. Acknowledgements

The students among the authors would like to thank their teachers Mr. Seidemann and Mr. Irmer for taking them to CERN and BESSY II and sharing their passion for physics with them. They would also like to thank Sarah Aretz and Margherita Boselli for organizing the competition as well as all volunteers from DESY and CERN for supporting the data analysis. The students are thankful for financial support by the Wilhelm and Else Heraeus Foundation, the Arconic Foundation, AMGEN, and the Ernest Solvay Fund, managed by the King Baudouin Foundation, that has been provided to BL4S through the CERN and Society Foundation. Reception of radiators from Thibaut Lefèvre of CERN and Heraeus Group is gratefully acknowledged. The measurements leading to these results have been performed at the Test Beam Facility at DESY Hamburg (Germany), a member of the

315 Helmholtz Association (HGF).

316 **6. Declaration of Competing Interest**

317 The authors declare that they have no known competing financial inter-
318 ests or personal relationships that could have appeared to influence the work
319 reported in this paper.

320 **7. Data availability**

321 Data will be made available on request.

322 **References**

- 323 [1] Cherenkov radiation,
324 <https://www.britannica.com/science/Cherenkov-radiation>,
325 (accessed on September 8th, 2022).
- 326 [2] P. A. Cherenkov, Visible radiation produced by electrons moving in
327 a medium with velocities exceeding that of light, *Physical Review* 52
328 (1937) 378.
- 329 [3] I. Tamm, Radiation emitted by uniformly moving particles, *Journal of*
330 *Physics* 1 (1939) 439–454.
- 331 [4] V. L. Ginzburg, I. M. Frank, Radiation of electrons and atoms moving
332 along the axis of a tube in a dense medium, *Sov. Phys. Dokl.* 56, 699
333 (1947).
- 334 [5] J. G. Linhart, Cherenkov radiation of electrons moving parallel to a
335 dielectric boundary, *J. Appl. Phys.* 26, 527 (1955). doi:[https://doi.](https://doi.org/10.1063/1.1722033)
336 [org/10.1063/1.1722033](https://doi.org/10.1063/1.1722033).
- 337 [6] R. Ulrich, Zur cherenkov-strahlung von elektronen dicht über einem
338 dielektrikum, *Z. Physik* 194, 180–192 (1966). doi:[https://doi.org/](https://doi.org/10.1007/BF01326045)
339 [10.1007/BF01326045](https://doi.org/10.1007/BF01326045).
- 340 [7] D. Harryman, et al., Properties of cherenkov diffraction radiation as pre-
341 dicted by the polarisation currents approach for beam instrumentation,
342 2020. doi:[10.18429/JACoW-IBIC2020-THPP05](https://doi.org/10.18429/JACoW-IBIC2020-THPP05).

- [8] K. Lasocha, et al., Simulation of cherenkov diffraction radiation for various radiator designs, 2020. doi:10.18429/JACoW-IBIC2020-TUPP28.
- [9] R. Kieffer, et al., Direct observation of incoherent cherenkov diffraction radiation in the visible range, Physical Review Letters 121 (2018) 054802. doi:10.1103/PhysRevLett.121.054802.
- [10] D. Alves, et al., Cherenkov diffraction radiation as a tool for beam diagnostics, in: Proceedings of IBIC2019, Malmö, Sweden, 2019. doi:10.18429/JACoW-IBIC2019-THA001.
- [11] L. Bobb, et al., Feasibility of diffraction radiation for noninvasive beam diagnostics as characterized in a storage ring, Physical Review Special Topics - Accelerators and Beams 21 (03 2018). doi:10.1103/PhysRevAccelBeams.21.032801.
- [12] T. Lefevre, et al., Non-invasive beam diagnostics with cherenkov diffraction radiation, IPAC 2018, JACoW Publishing (2018). doi:10.18429/JACoW-IPAC2018-WEPAF074.
- [13] M. Shevelev, A. Konkov, Peculiarities of the generation of vavilov-cherenkov radiation induced by a charged particle moving past a dielectric target, J. Exp. Theor. Phys. (2014). doi:10.1134/S1063776114030182.
- [14] R. Kieffer, et al., Generation of incoherent cherenkov diffraction radiation in synchrotrons, Physical Review Accelerators and Beams 23 (04 2020). doi:10.1103/PhysRevAccelBeams.23.042803.

- [15] A. Curcio, et al., Noninvasive bunch length measurements exploiting cherenkov diffraction radiation, *Physical Review Accelerators and Beams* 23 (02 2020). doi:10.1103/PhysRevAccelBeams.23.022802.
- [16] E. Arce-Larreta, et al., Behind the scenes: The two-weeks stay of beamline for schools winning students at desy, *The Physics Educator* 03 (2021) 2150001. doi:10.1142/S2661339521500013.
- [17] S. Aretz, et al., An overview of the cern beamline for schools competition, *The Physics Educator* 02 (2020) 2050001. doi:10.1142/S2661339520500018.
- [18] R. Diener, et al., The desy ii test beam facility, *Nuclear Instruments and Methods in Physics Research Section A: Accelerators, Spectrometers, Detectors and Associated Equipment* 922 (12 2018). doi:10.1016/j.nima.2018.11.133.
- [19] H. Jansen, et al., Performance of the eudet-type beam telescopes, *EPJ Techn Instrum* 3, 7 (2016). doi:https://doi.org/10.1140/epjti/s40485-016-0033-2.
- [20] Et enterprises pmt 9113b series, <https://et-enterprises.com/products/photomultipliers/product/p9813b-series>, (accessed on October 31th, 2022).
- [21] Heraeus, <https://www.heraeus.com/en/group/home/home.html>, (accessed on September 8th, 2022).
- [22] P. Baesso, D. Cussans, J. Goldstein, The aida-2020 flu: a flexible trigger

- 387 logic unit for test beam facilities, Journal of Instrumentation (2019).
388 doi:10.1088/1748-0221/14/09/p09019.
- 389 [23] Caen, <https://www.caen.it/products/v965/>, v965, 16 Channel Dual
390 Range Multievent QDC.
- 391 [24] Y. Liu, et al., EUDAQ2—a flexible data acquisition software frame-
392 work for common test beams, Journal of Instrumentation 14 (10) (2019)
393 P10033–P10033. doi:10.1088/1748-0221/14/10/p10033.
- 394 [25] Root version 6.24.06, cern, <https://root.cern/>, (accessed on Septem-
395 ber 8th, 2022).
- 396 [26] Jupyter notebook python 3.6.8, <https://jupyter.org/>, (accessed on
397 September 8th, 2022).
- 398 [27] H. Jansen, P. Schütze, Feasibility of track-based multiple scattering to-
399 mography, Appl. Phys. Lett. 112, 144101 (2018). doi:[https://doi.](https://doi.org/10.1063/1.5005503)
400 [org/10.1063/1.5005503](https://doi.org/10.1063/1.5005503).
- 401 [28] M. Q.-M. J. Arling, C. David, Radiation length measurements for
402 the atlas itk strip detector, [https://indico.desy.de/event/18050/](https://indico.desy.de/event/18050/contributions/28728/attachments/18386/23522/MBI_ATLAS_BTtB6.pdf)
403 [contributions/28728/attachments/18386/23522/MBI_ATLAS_](https://indico.desy.de/event/18050/contributions/28728/attachments/18386/23522/MBI_ATLAS_BTtB6.pdf)
404 [BTtB6.pdf](https://indico.desy.de/event/18050/contributions/28728/attachments/18386/23522/MBI_ATLAS_BTtB6.pdf), (accessed on October 31th, 2022).
- 405 [29] D. Dannheim, et al., Corryvreckan: a modular 4d track reconstruction
406 and analysis software for test beam data, Journal of Instrumentation 16
407 (2021). doi:10.1088/1748-0221/16/03/p03008.

- 408 [30] L. Moneta, Errorintegral.c file root reference, [https://root.cern/doc/](https://root.cern/doc/master/ErrorIntegral_8C.html)
409 [master/ErrorIntegral_8C.html](https://root.cern/doc/master/ErrorIntegral_8C.html), (accessed on October 31th, 2022).

Declaration of interests

☒ The authors declare that they have no known competing financial interests or personal relationships that could have appeared to influence the work reported in this paper.

☐ The authors declare the following financial interests/personal relationships which may be considered as potential competing interests: